Original Paper

Chemical interactions between monomer and template in molecularly imprinted polymers, the EGDMA:2-VP (4:1) - lumefantrine MIP case study

Maria Betânia de Freitas-Marques[1,2]*, Pedro Henrique Reis da Silva[2], Tércio Assunção Pedrosa[3], Maria Irene Yoshida[1], Christian Fernandes[2], Wagner da Nova Mussel[1]

[1] Departamento de Química, Instituto de Ciências Exatas, Universidade Federal de Minas Gerais - UFMG, Av. Antônio Carlos 6627, Belo Horizonte, Minas Gerais, Brazil.*e-mail: betanialf@hotmail.com.

[2] Faculdade de Farmácia, Universidade Federal de Minas Gerais - UFMG, Av. Antônio Carlos 6627, Belo Horizonte, Minas Gerais, Brazil.

[3] Laboratório de Microscopia Eletrônica, Centro de Desenvolvimento da Tecnologia Nuclear – CDTN, Av. Antônio Carlos 6627, Belo Horizonte, Minas Gerais, Brazil.

_____‡‡_____

Abstract. Molecularly Imprinted Polymers (MIP) are synthetic materials used as a tool to enhance the selectivity in different analytical approaches, such as solid-phase extraction, chromatography, and sensing devices. Knowing the mechanism involved in the interaction between the template and monomer is essential for a further successful application. However, studies on this topic are scarce. This work evaluates the involved mechanisms in the template-monomer interaction for a lumefantrine MIP system, an antimalarial drug. Field-emission gun scanning electron microscopy, thermal analysis, X-ray diffraction, and density functional theory were applied to determine the mechanism involved in two MIPs obtained in different conditions. A new parameter, named Molecularly Imprinting Factor (MIF), was proposed to evaluate the contribution of specific interactions in the sorption of the analyte by the MIP structure. MIF allows direct insights into specific binding, non-specific contributions, interaction nature, behavior predictability, system acid-base behavior, pre-screening pairs capability, and binding site affinities evaluation. Two sorts of interaction were observed, covalent and non-covalent when methacrylic acid and 2-vinyl pyridine were used as monomers, respectively. Therefore, the use of methacrylic acid formed a sorbent inappropriate for solid-phase extraction since the binding is not reversible. On the other hand, 2-vinyl pyridine-lumefantrine binding was reversible, and MIF = 0.59 (59.02% of specific site sorption) indicates that the predominant mechanism in the sorption is specific.

Keywords: Molecularly imprinting factor, an antimalarial drug, thermal behavior, glass transition, element mapping, sorption mechanism

_____

1. Introduction

Molecularly Imprinted Polymers (MIPs) are synthetic materials used to enhance selectivity in different analytical approaches, such as solid-phase extraction, chromatography, and sensing devices [1–4]. MIPs are synthesized by polymerizing functional monomers and crosslinkers around a template, which can be the analyte of interest itself (drug, metabolites, ambient undesirable compounds such as pesticides, harmonious, and so on) or a structural analog molecule, leading to the cross-linked formation of three-dimensional selective cavities of equivalent size shape, and chemical affinity. After removing the template, cavities are available for selectively binding the target analyte from different samples [5–7].

The overall production of a molecularly imprinted polymer comprises three main steps: (i) formation of covalent or non-covalent contacts between template and functional monomer molecules, (ii) polymerization itself (under some specific conditions) and, finally, (iii) template removal from the target-specific synthetic polymer [3,8].

The interaction between monomer and template can be covalent, non-covalent, or semi-covalent. In the covalent approach, these bonds may form during MIP synthesis or in the course of its analytic use for extraction. The kinetic involved in establishing a covalent bond is slow. Therefore, this mechanism is not used for MIP synthesis [9]. In a non-covalent approach, interactions like hydrogen bonding, van der Waals forces, π-π and hydrophobic interactions, electrostatic forces, and metal coordination are formed [3,5,12]. The non-covalent approach is the preferred mechanism used in MIP synthesis due to its simplicity, the versatility of the compounds that can be imprinted, and the variety of commercially available functional monomers [10]. Another approach is semi-covalent, which is a combination of covalent and non-covalent mechanisms. In this case, the interaction between the monomer and the template molecule before the polymerization is covalent, whereas the analyte binding during the polymer's use is non-covalent, such as the interaction between 2-vinyl pyridine and lumefantrine as described by Silva et al. (2018) [7,9,10]. Chemical interactions between monomer and template are fundamental for determining the molecularly imprinting factor (MIF), which attests to the performance of MIP [11].

MIPs are mainly used as sorbent in solid-phase extraction (SPE) and their variations, in the solid-phase microextraction, microextraction by packed sorbent, and dispersive solid phase extraction [6,8,10,12–14] in different matrices, including biological fluids [4,5,7,15],

food [16,17], supplements [18] and environmental samples [19,20]. The choice of appropriate reagents (monomer, crosslinker, porogenic solvent, and radical initiator) is essential to establish suitable characteristics based on morphology, stability, binding, and selectivity [11,21,22]. Moreover, the stereochemistry of template and polymerization conditions are determinants for obtaining an adequate MIP [2,3,12,23]. Rational design of molecularly imprinted polymers for the analyte recognition englobe the possibility of structure-property relationship studies described by Fernandes and colleagues (2015) [24]. Analytical experiments for appropriate monomers screening to the template as described by Roy and colleagues (2018) [25] may be used to optimize the conditions for the MIP synthesis and avoid excessive experiments that are burdensome and time-consuming.

In this context, thermal analysis and X-ray diffraction is powerful tool for a complete understanding of MIP properties [26,27]. Understanding the thermal behavior provides essential information about solid-state properties that control the molecular system organization and its surrounding physicochemical interactions.

The present study evaluates the type of interaction between template and monomer in a MIP for lumefantrine, an antimalarial drug. Different techniques were applied: thermal analysis, field-emission gun scanning electron microscopy, and X-ray diffraction. Even though several MIPs have been synthesized to be applied in SPE, few studies discuss the mechanism involved in template-monomer binding during the overall process.

2. Experimental section

2.1. Samples

Several MIPs candidate for lumefantrine were synthesized. Different combinations of monomer (2-hydroxyethyl-methacrylate, 2-vinyl pyridine, and methacrylic acid), crosslinker (divinylbenzene, ethylene glycol dimethacrylate, and trimethylolpropane trimethacrylate), and porogenic solvent (ethyl acetate, chloroform, and toluene) were evaluated. The performance tests are a demanding evaluation for each considered pair. The polymers were synthesized using the precipitation polymerization method. The summarized conditions are shown in Table 1. Detailed data is present in a previous study developed by our group [7].

Table 1. Conditions employed in the synthesis of MIP for lumefantrine, as described by Silva et al. (2018) [7].

MIP	Composition			Molar proportion*
	Functional monomer	**Crosslinker**	**Porogenic solvent**	
1	2-HEMA	TRIM	TOL	01:04:20
2	2-HEMA	DVB	TOL	01:04:20
3	2-VP	TRIM	TOL	01:04:20
4	2-VP	DVB	TOL	01:04:20
5	2-HEMA	EGDMA	CLO	01:04:20
6	2-HEMA	EGDMA	ETAC	01:04:20
7	2-VP	EGDMA	CLO	01:04:20
8	2-VP	EGDMA	ETAC	01:04:20
9	MAA	TRIM	CLO	01:04:20
10	MAA	TRIM	ETAC	01:04:20
11	MAA	DVB	CLO	01:04:20
12	MAA	DVB	ETAC	01:04:20
13	MAA	EGDMA	TOL	01:04:20
14	2-VP	EGDMA	TOL	01:06:30

2-HEMA: 2-hydroxyethyl methacrylate; 2-VP: 2-vinyl pyridine; MAA: methacrylic acid; DVB: divinylbenzene; EGDMA: ethylene glycol dimethacrylate; TRIM: trimethylolpropane trimethacrylate; ETAC: Ethyl acetate; CLO: chloroform; TOL: toluene. *Molar proportion - lumefantrine: functional monomer: crosslinker

The MIP-14 and MIP-9 were chosen as examples to discuss the mechanisms involved in template-monomer binding since they have distinct behavior in terms of template-monomer interaction.

Distribution coefficient (K_D), equation 1, was used to calculate the specific binding factor due to molecularly imprinting related to the total binding (specific and non-specific), using equation 2. Therefore, the molecularly imprinting factor (MIF) was defined to describe the chemical interactions.

$$K_D = \frac{(C_i - C_f) \times V}{m}$$ **Equation 1**

Ci and *Cf* are the initial and final concentrations of a solution containing lumefantrine at 24 µg/mL, *V* is the volume (5 mL), and *m* is the MIP mass (50 mg). K_D was obtained through adsorption studies [7].

$$MIF = \frac{K_D(imprinted) - K_D(non-imprinted)}{K_D(imprinted)}$$ **Equation 2**

K_D *(imprinted)* is the molecularly imprinted polymer's distribution coefficient, and K_D *(non-imprinted)* is the distribution coefficient of the non-imprinted polymer.

2.2. Field Emission Gun - Scanning Electron Microscopy (FEG-SEM)

A Field Emission Gun - Scanning Electron Microscope (FEG-SEM) SIGMA VP model from Carl Zeiss Microscopy GmbH coupled with a Bruker Gmbh EDS XFlash 410-M detector was used to perform microstructural and element mapping chemical characterization. FEG-SEM was performed for lumefantrine API, MIP-9, MIP-9 submitted to 0.1 M HNO_3 and 0.1 M HCl, MIP-14, and MIP-14 lumefantrine-loaded (MIP-14-T).

2.3. Thermal Analysis

Differential Scanning Calorimetry (DSC) curves were obtained in the DSC60 Shimadzu under a dynamic nitrogen atmosphere, with a flow rate of 50 mL min^{-1}, a heating rate of 10 °C min^{-1} from room temperature up to 400 °C in a closed aluminum crucible. Samples were about 1.5 mg, accurately weighted. The results are in J g^{-1}. Lumefantrine, MIP-9, MIP-14, MIP-14-T, physical mixture containing lumefantrine + MIP-14 (1:0.4 w/w) and NIP were analyzed by DSC.

The experimental determination of glass transition (Tg) was conducted by DSC as described by the American Society for Testing and Materials, ASTM D3418 – 15 [28]. The Synthia routines were used for Tg theoretical calculations. This method allows rapid estimates of polymer properties using empirical and semiempirical methods [29,30].

2.4. X-ray diffraction

Powder X-ray diffraction (PXRD) data were collected using an XRD-7000 diffractometer Shimadzu operated at 20 °C, 40 kV, and 30 mA, using CuKα (λ= 1.54056 Å) equipped with a polycapillary focusing optics under parallel geometry coupled with a graphite monochromator. The acquired samples were read under spinning at 60 rpm, to prevent any preferred orientation, scanned over an angular range of 4 - 60° (2θ) with a step size of 0.02° (2θ) and a time constant of 2 s/step. PXRD was obtained for lumefantrine, MIP-14, and a physical mixture containing lumefantrine + MIP-14 (1:0.4 w/w).

2.5. Density Functional Theory (DFT) calculations

A detailed explanation of DFT expressions is given by Di Carlos, A. et al. [31]. The fundamental step of the DFTB+ derivation is to expand the total energy of the DFT representation to the second-order in charge density and spin density fluctuations by Elstner, M. et al. [32]. The first-principles calculations were performed by density functional theory (DFT) [33,34]. Were used Troullier_Martin norm-conserving relativistic pseudopotentials [35] in Kleinman_Bylander's nonlocal form [36]. The treatment of exchange and correlation

energies within the generalized gradient approximation takes place according to the Perdew, Burke, and Ernzerhof (PBE) parametrization [37]. The split valence and perturbative polarization methods were employed to generate a double-zeta basis for each angular momentum plus polarization orbitals (the standard SIESTA DZP basis set). A minimal 200 Ry mesh-cutoff energy was applied to determine real space grid fineness.

3. Results and discussion

The imprinting factor (IF) is a parameter that expresses the efficiency of the template-functional monomer binding. Therefore, a strong interaction inside the MIP would yield a high imprinting factor, while weak interactions would lead to small calculated imprinting factors.

The IF factor found in the literature [38] is calculated as described in equation 3. It indicates the relationship between the sorption capacities of MIP and NIP. However, it does not show clearly the type of sorption involved in the molecularly imprinting process.

$$IF = \frac{K_D(imprinted)}{K_D(non-imprinted)} \qquad \textbf{Equation 3}$$

This study proposes a new parameter, MIF, which directly shows the specific binding preference related to the total binding (specific and non-specific sites). The sorption occurring in MIP is due to specific and non-specific interactions. When the contribution of non-specific binding is removed, the interaction provided by specific sites (molecularly imprinting) can be directly accessed. Therefore, the proposed MIF allows the unambiguous identification of the preferred mechanism of sorption in the MIP. Table 2 shows the comparison between the accessed properties obtained by the conventional imprinting factor (IF) and the proposed molecularly imprinting factor (MIF).

Table 2. Comparison between the accessed properties obtained by the conventional imprinting factor (IF) and the proposed molecularly imprinting factor (MIF).

Properties	IF	MIF
Specific binding	X	X
Non-specific contributions	-	X
Interaction nature	-	X
Behavior predictability	-	X
System acid-base behavior	-	X
Pre-screening pairs capability	-	X
Binding site affinities	-	X

The MIF factor allows obtaining specific information from the studied system. Behind the specific binding information extracted from both, the proposed MIF factor explores the non-specific contributions, acting in the system, since the non-imprinted information is subtracted. The result is the specific net effect information over significant system characteristics. That allows working with the nature of the interaction since the involved species are a weak acid and bases compounds. By this information, the acid-base system behavior is predictable as far as the attractive or repulsive affinities can be understood and controlled, giving rise to unparallel predictability of the proposed pair components. The screening of the best pre-defined pairs to improve efficiency is theoretically evaluated previously to laboratory tests. There is a significant decrease in time and laboratory costs involved in the design, test, and definition of the best pair combination to the optimum results. The costly and time-consuming combinatory analysis is eliminated by the pre-screening of the best chemical pairs. It is imperative to understand the chemical interactions between monomer and template in a molecularly imprinted polymer.

For instance, a set of MIPs for lumefantrine (Table 3) shows the K_D (imprinted), K_D (non-imprinted), IF, MIF, and %MIF (for MIF positive values) for the 14 synthesized MIPs.

Table 3. K_D (imprinted), K_D (non-imprinted), IF, MIF, and %MIF.

MIP	K_D (imprinted)	K_D (non-imprinted)	IF	MIF	%MIF
1	540.96	1080.99	0.50	-0.998	-
2	558.3	561.17	0.99	-0.005	-
3	1022.41	656.23	1.56	0.358	35.82
4	583.73	348.14	1.68	0.403	40.36
5	718.79	777.82	0.92	-0.082	-
6	595.74	564.6	1.06	0.005	5.23
7	649.04	535.3	1.21	0.175	17.52
8	598.87	344.24	1.74	0.425	42.52
9	244.51	669.38	0.37	-1.737	-
10	566.78	1246.87	0.45	-1.199	-
11	918.14	939.6	0.98	-0.002	-
12	922.1	934.74	0.99	-0.013	-
13	773.32	703.76	1.10	0.089	8.99
14	977.83	400.75	2.44	0.590	59.02

Only for some systems, the sorption of lumefantrine at specific MIP sites predominates. This behavior characterizes the molecular impression. For the other systems, the contribution of non-specific interactions is predominant. The closer the MIF value is to 1, the greater the sorption at specific sites, indicating effectiveness in the proposed molecular

impression's synthesis process. The sign is related to a permanent covalent interaction. As closer as to -1 relates to non-specific site interaction. The difference is positive MIF factor indicates a predominance of reversible bonding, whereas the negative indicates the predominance of permanent bounding. This explanation is summarized in Table 4.

Table 4. MIF range explanation.

Range	Phenomenon
MIF = 1	Only specific site sorption (MIP) – the NIP contribution is equals to zero
0 < MIF < 1	Specific site sorption is predominant (MIP)
MIF = 0	Specific (MIP) and non-specific (NIP) have equaled sorption contributions.
MIF < 0	Non-specific site sorption is predominant (NIP)

The MIF for MIP-14 was 0.59, corresponding to 59% of specific site sorption. As previously discussed, the MIF value indicates a factor straight related to the specific and non-specific analyte-MIP interaction. Therefore, the sorption mechanism in MIP-14 is preferentially on the specific sites since 0 < MIF < 1, showing that molecularly imprinting behavior was achieved in the synthesis.

The MIP-9 (MIF = -1.737, therefore MIF <0) comprises lumefantrine, methacrylic acid (MAA), and trimethylolpropane tri-acrylate (TRIM). The MAA monomer is an organic acid, and lumefantrine has a basic nature; therefore, a strong acid-base neutralization reaction is expected. A FEG-SEM experiment monitored by their atomic numbers was performed for topography images of the polymer surface distribution. Fig. 1a shows MIP-9 after template removal, performed in a Soxhlet with chloroform. Lumefantrine was still present, as observed by the chlorine (yellow color), exclusively present in the lumefantrine molecule. For lumefantrine remotion, the polymer was transferred to a flask, 0.1 M HNO_3 and 0.1 M HCl were added separately, and the suspension was stirred for 5 minutes. Nevertheless, as evidenced by the images (Fig. 1b and c), lumefantrine was not removed from the MIP surface.
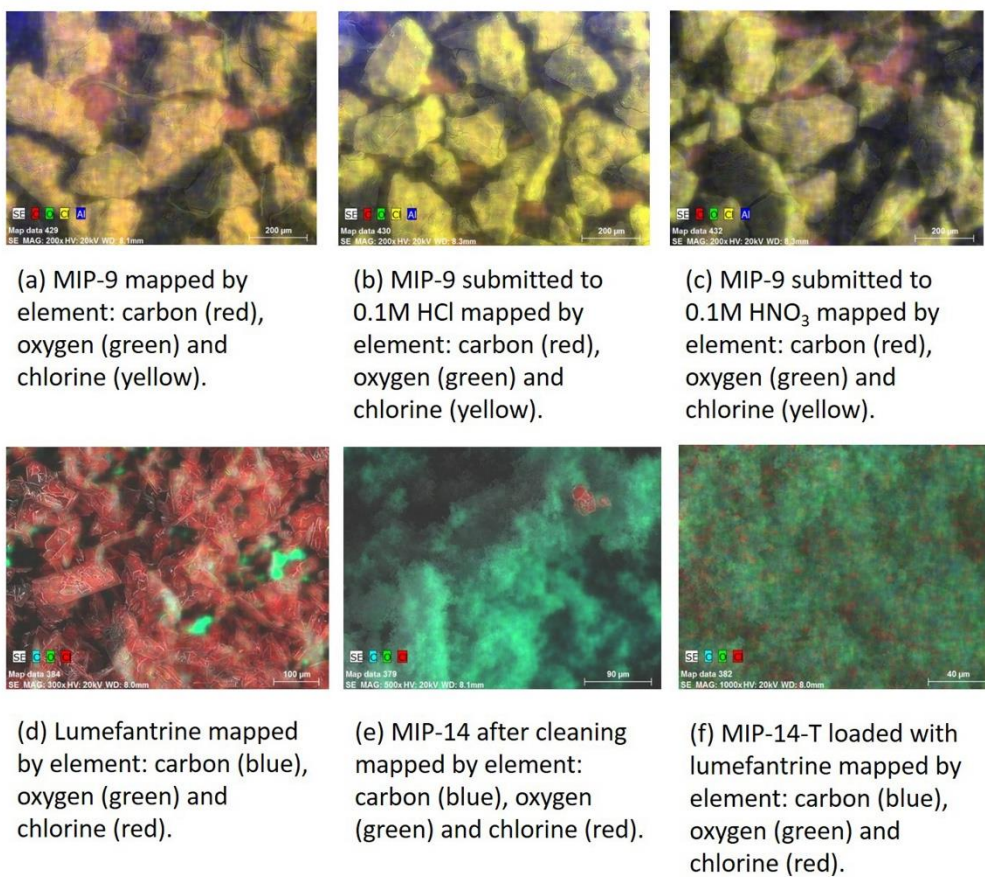
(a) MIP-9 mapped by element: carbon (red), oxygen (green) and chlorine (yellow).

(b) MIP-9 submitted to 0.1M HCl mapped by element: carbon (red), oxygen (green) and chlorine (yellow).

(c) MIP-9 submitted to 0.1M HNO$_3$ mapped by element: carbon (red), oxygen (green) and chlorine (yellow).

(d) Lumefantrine mapped by element: carbon (blue), oxygen (green) and chlorine (red).

(e) MIP-14 after cleaning mapped by element: carbon (blue), oxygen (green) and chlorine (red).

(f) MIP-14-T loaded with lumefantrine mapped by element: carbon (blue), oxygen (green) and chlorine (red).

Fig. 1. A Field Emission Gun - Scanning Electron Microscope (FEG-SEM) for MIP-9 (a), MIP-9 submitted to 0.1M HCl (b) and 0.1M HNO$_3$ (c), lumefantrine (d), MIP-14 (e) and MIP-14 lumefantrine-loaded (MIP-14-T) (f).

The FEG-SEM images obtained for MIP-9 suggest that the interaction between lumefantrine (template) and MAA (monomer) occurs through covalent bonding. Density Functional Theory (DFT) was employed to simulate the low energy configuration, where the binding template-monomer occurs spontaneously. This condition is achieved when the carboxylic radical and hydroxyl group were near each other, as observed in the scheme (Fig. 2). Therefore, the DFT simulation corroborates the covalent bond hypothesis between lumefantrine and MAA, resulting in the permanent immobilization of lumefantrine in the polymer chain.

This behavior agrees with the observed negative MIF (-1.737) value for MIP-9 (Table 2), indicating a predominant non-specific adsorption mechanism since the value of K_D for NIP was about three times higher than the MIP. Therefore, the binding between MAA and LUM, irreversible, forms a stable system, making it impossible to be used as a sorbent for solid-phase extraction. The template molecule definitively occupies the binding sites for the analyte.
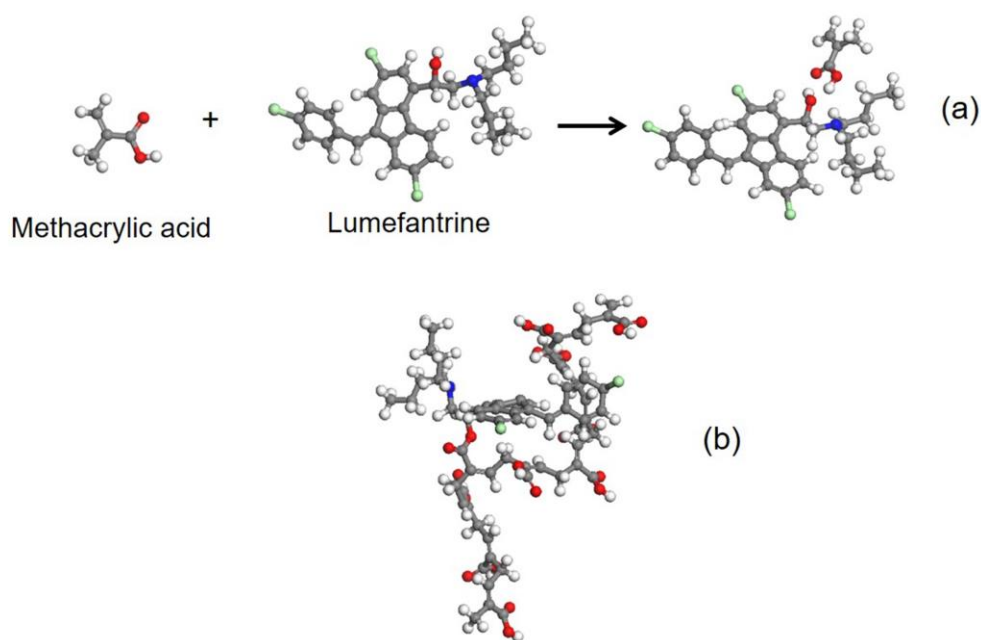
Fig. 2. (a) Density Functional Theory (DFT) simulation for methacrylic acid (MAA) + lumefantrine (LUM) interaction; (b) lumefantrine docked in methacrylic acid polymer chain.

FEG-SEM EDS coupled was also performed for lumefantrine and MIP-14 (Figure 1, d, e, and f). Lumefantrine, monitored by chlorine (red color), is shown in Fig. 1d. Figure 1e shows template removal after Soxhlet, evidencing the reversible character of the lumefantrine-monomer binding. The observed red spot is related to a residual lumefantrine over the surface, confined in a restricted region. After loading MIP-14 with lumefantrine (MIP-14-T, Fig. 1f), the chlorine (red color) homogeneity spread all over the polymer surface.

The interaction between the template and the monomer (2-vinyl pyridine) is reversible, non-covalent, as observed through DFT simulation. A hypothesis is the hydrophobic binding between the 2-vinyl pyridine ring and lumefantrine rings (Fig. 3a). Therefore, this MIP can be used as a sorbent in SPE since it can restore the sorption capability after each extraction. Fig. 3b shows the DFT simulation for the interaction between 2-vinyl pyridine (functional monomer of MIP-14) and lumefantrine in higher energy configuration (closest molecules). Computational approximations between all components system (template, functional monomer, crosslinker, and porogen) play a key role in obtaining the best combinations for molecularly imprinted polymers. This approach can narrow the search space to just a few optimum combinations, making the screening of

reagents and conditions more manageable, economical, and easy to be confirmed empirically in a laboratory setting, as described by Liu and colleagues [39].
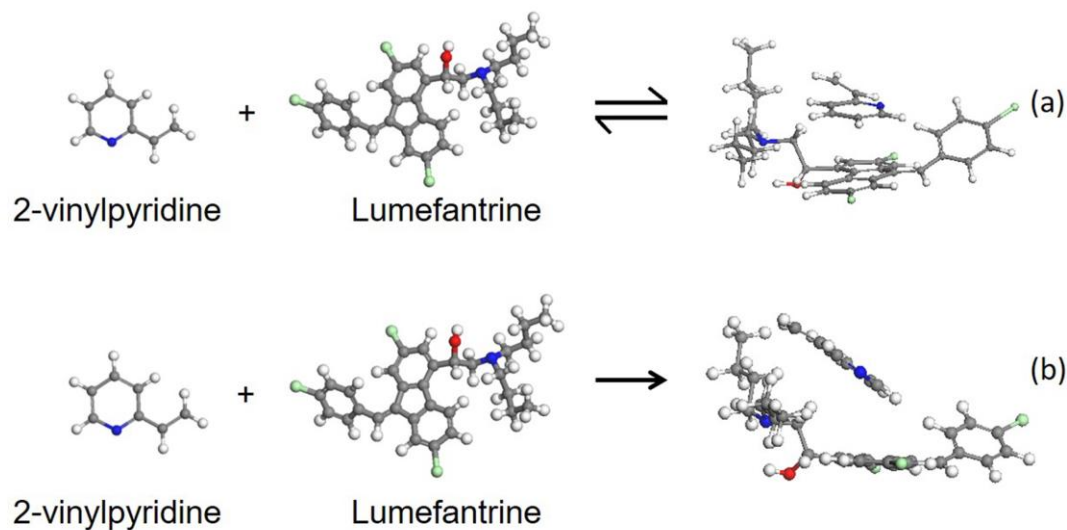

Fig. 3. Density Functional Theory (DFT) simulation for 2-vinylpyridine (2-VP) + lumefantrine (LUM) interaction. (a) lower and (b) higher energy configuration.

A relevant aspect to be considered in the polymerization process of MIP is the possibility of a chemical reaction between the template and other system components. Based on that possibilities, thermal analysis experiments and X-ray diffraction were conducted, searching for evidence. Fig. 4 shows the DSC curves for lumefantrine (LUM), MIP-14, and lumefantrine-loaded MIP-14 (MIP-14-T). The dotted line at 128.1 ºC (T_{onset}) shows the lumefantrine's melting event, as expected [40]. DSC curve for MIP-14 shows an endothermic event at 53 ºC, related to the residual solvent loss (confirmed by thermogravimetry, data not shown).

Interestingly, the DSC curve for MIP-14-T did not show the thermal behavior of lumefantrine or MIP-14, suggesting an interaction between LUM and MIP occurs when heat is provided to the system. If LUM molecules were chemically linked through Van der Waals or hydrogen bonding forces, the fusion event for LUM would be observed alone. Therefore, supported by the DSC experiment, a new entity was formed. It is the product of the reaction between lumefantrine and the other components from MIP-14 under heating.
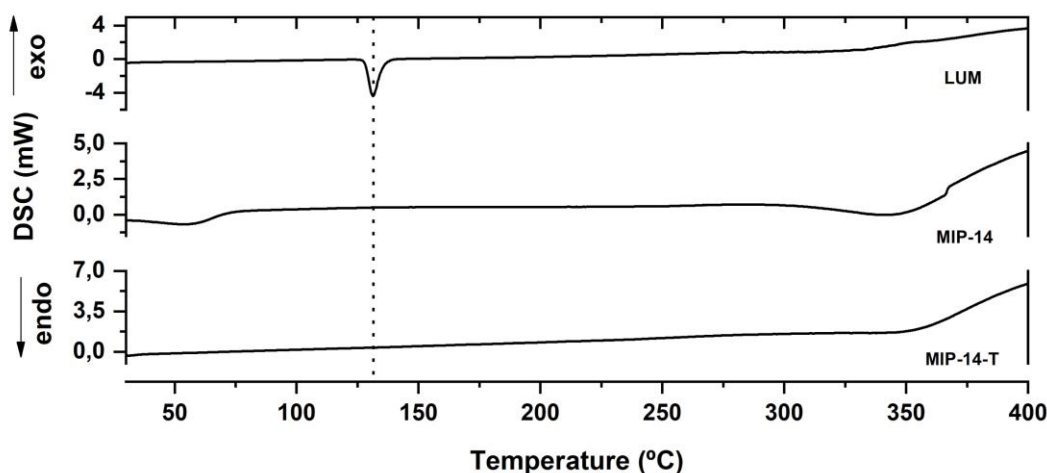
Fig. 4. DSC curves for lumefantrine (LUM), pure polymer 14 (MIP-14), and lumefantrine-loaded MIP-14 (MIP-14-T).

Fig. 5 shows an endothermic peak at 128.1 ℃ (T_{onset}) in the DSC curve, related to the lumefantrine melting, confirmed by its X-ray diffraction fitted by the Rietveld method. For MIP-14, the DSC curve shows an endotherm peak at about 57 ℃ due to solvent loss; the X-ray diffraction shows its amorphous nature. Afterward, lumefantrine and MIP-14 were separately submitted to heating, running up 150 ℃, cooling down to room temperature, and heating up again to 150 ℃. The observed melting temperature was 124.9 ℃ (T_{onset}) for lumefantrine, lower than that obtained in the first run (128.1 ℃). This slight difference is related to the loss of unit cell organization, probably due to changes in the intermolecular forces, confirmed by X-ray diffraction. For MIP-14, the first heating cleaned the "thermal history," as seen in the respective DSC and X-ray diffraction. The same experiment was conducted in a physical mixture containing MIP-14 and lumefantrine (1:0.4 w/w) to evaluate the thermal behavior of this mixture. The exothermal peak at about 170 ℃ in the DSC curve and new peaks at 16 and 33º 2θ in the diffractogram confirmed a new entity's formation. The entity is formed by crystallization since these signals were observed neither in lumefantrine nor in MIP-14 when evaluated alone. Freitas-Marques et al. (2020) determined the non-isothermal kinetic study of the interaction between lumefantrine and molecularly imprinted polymer for this new entity [26].
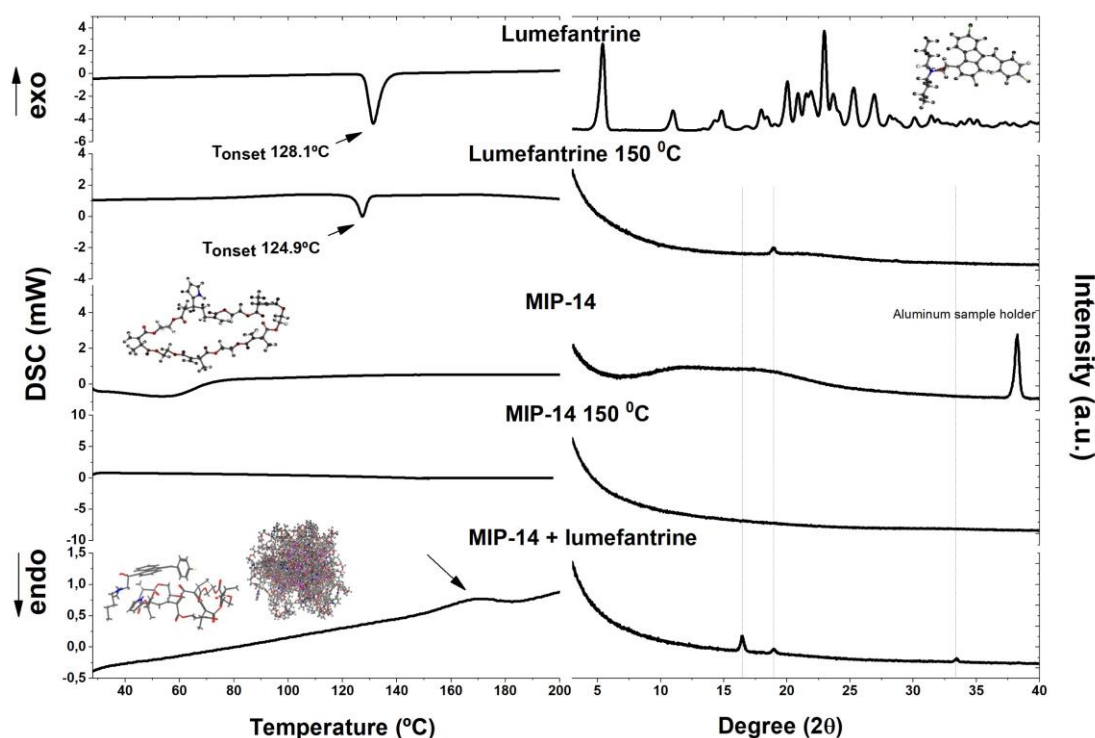
Fig. 5. DSC (left) and X-ray diffraction (right) of lumefantrine; MIP-14; MIP-14 heated 150 ℃, cooled down to room temperature and heated 150 ℃ again; lumefantrine heated 150 ℃, cooled down to room temperature and heated 150 ℃ again; and MIP-14 + lumefantrine (1:0.4 w/w) physical mixture heated 150 ℃, cooled down to room temperature and heated 200 ℃ again.

To the best of our knowledge, it is essential to emphasize that the determination of glass transition (Tg) for MIP does not exist in the literature. In an unprecedented way, the determination of Tg for MIP-14 was proposed in this research. This information is helpful in materials processing technology because from the glass transition temperature, the molecules lose rigid or semi-crystalline arrangement and assume a more malleable state. Therefore mechanical properties can be modified to optimize molecularly imprinted polymer morphology and recognition.

Tg determination by DSC follows the requirements of the ASTM D3418-15. The sample was heated at 20 ℃.min^{-1} to 250 ℃ and kept in an isotherm for 10 minutes. This first heat treatment cycle is for cleaning the polymer "thermal history". Subsequently, the sample was cooled down to -60 ℃ and heated up again to 400 ℃. This second heating cycle is likely to observe the baseline shift characteristic of the glass transition in polymers. The baseline DSC curve of MIP-14 (second heating) shows four fluctuations, suggesting the glass transition observation (Fig. 6A). It is observed that the baseline shift was subtle. In an attempt to confirm this thermal phenomenon, the sample residues of second heating by DSC were collected before (T_{eig} = extrapolated onset temperature) and after (T_{efg} = extrapolated end

temperature) baseline shift of first and last doubtful points, been subsequently analyzed by XRD (Fig. 6B).
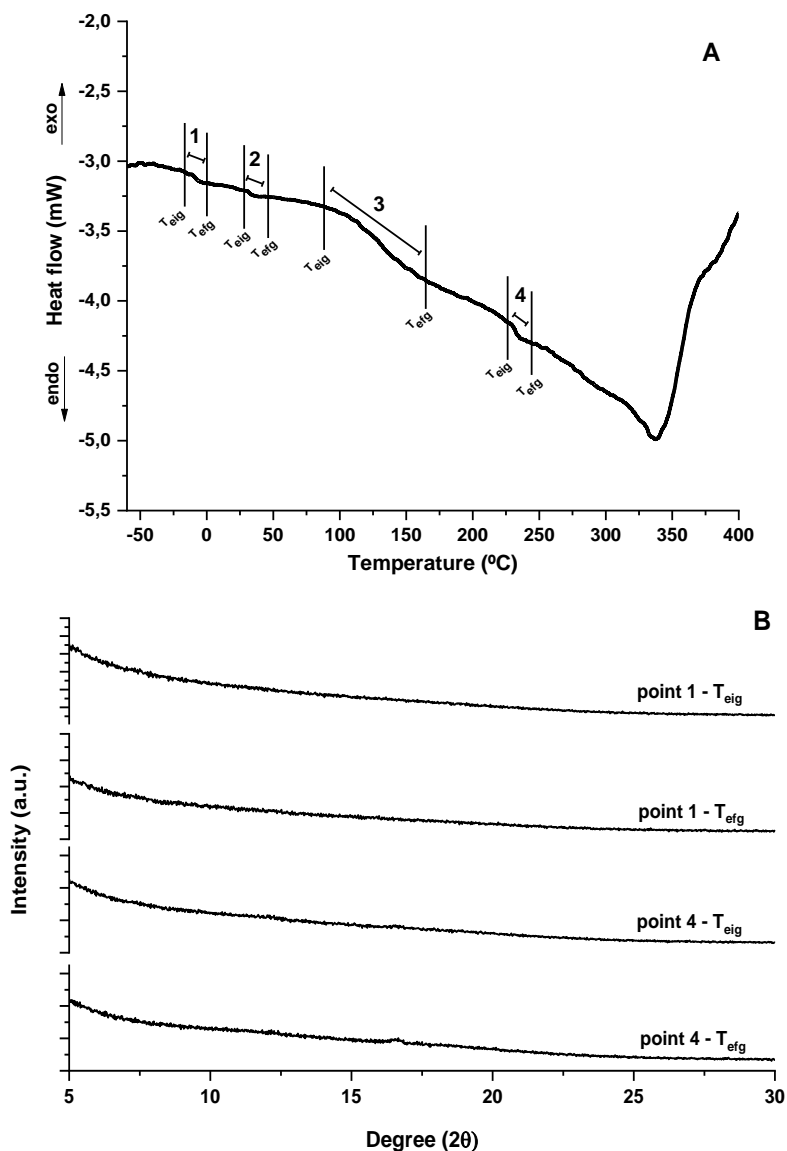

Fig. 6. Glass transition determination of MIP-14. DSC curve (A), second heating cycle, and powder X-ray diffraction (B) of sample residues before (T_{eig} = extrapolated onset temperature) and after (T_{efg} = extrapolated end temperature) baseline shift of 1 and 4 points.

As observed, PXRD shows no significant differences in the structural arrangement of MIP-14 to be identified as the glass transition of this type of polymer. Therefore, Synthia's method was proposed for topological information about polymers, instead of group contributions, in the predictive correlations, circumventing the limitation of the polymers that contain group contributions that conventional methods cannot estimate, as MIP-14, once chain and sequence lengths are other factors which can influence the thermal properties [41].

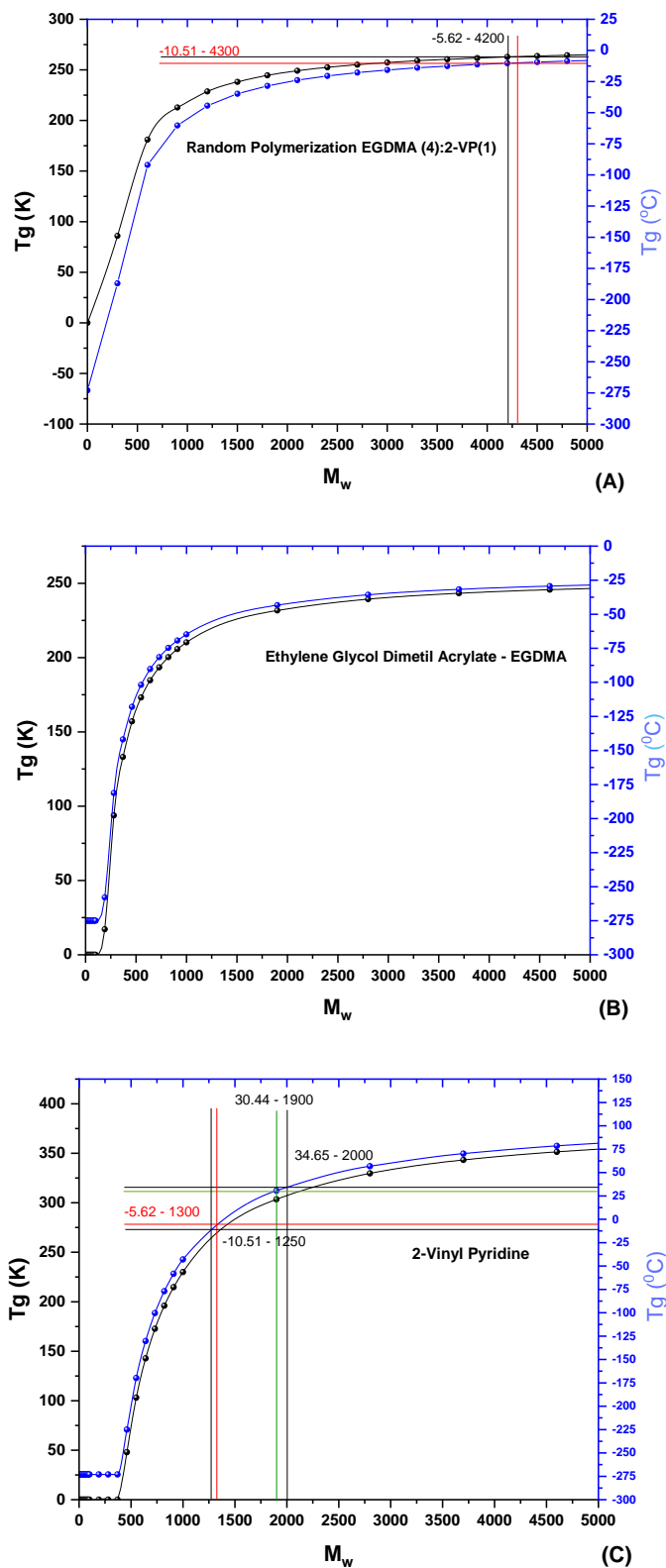Fig. 7 shows Tg prediction for EGDMA -2-VP (4:1) (A), free EGDMA (B), and 2-VP (C) by Synthia's method.

Fig. 7. Synthia© package glass transition prediction for EGDMA-2-VP (4:1) (A), EGDMA (B), and 2-VP (C).

The Tg will depend on the polymer molecular weight MW (amu) for linear polymers. Considering the structure of the homo or copolymer, the end of the polymer chain tends to be more flexible than the rest of the chain. By considering the chain increase, the molecular weight increases and, therefore, the mobility.

The plateau in the T_g x MW graphic results from the relatively rigid final polymer macrostructure configuration. Generally speaking, all factors such as lower flexibility, bulkier groups, cross-linking, intense chain interactions that may affect molecular mobility on a large scale have an increased effect over T_g.

However, as the polymer chain increases, the overall mobility will reduce up to a stable value as M_w increases; the phenomenon is usually associated with the "infinite Tg temperature". When reached the effect saturation, the Tg does not change with a further increase of MW usually after Mw 5000 – 10000 amu [42].

There are many industrial situations where formulators mix two polymers to produce a blend with improved physical properties. As far as pharmaceutical polymers are concerned, they are composed of small molecules. If used in a mixture, an essential concern property would be the miscibility when more than one monomer is present. If two monomers are still in a mixture, the cooling behavior is critical in interpreting the thermal curve. At cooling, the overall miscibility is complex, being limited on several occasions by the solubility limit of the active small molecules. Therefore, for a blend of two immiscible components, each phase will separately become vitreous if enough fast cooling rate is applied. In the DSC experiment, two distinct thermal phenomena will be observed, corresponding to the mixture's two pure compounds. Otherwise, only one T_g should be observable in the glassy blend characterization for an utterly miscible mixture.

For partially miscible blends, the expected behavior is somehow intermediate, with hard to identify thermal phenomenon due to the small amounts, tiny DH variations that rise from the imposed dilution, or the temperature range effect's superposition.

Four ranges of effects are observable in the Tg DSC experiment (Fig. 6A). The first one, ranging from -10.5 up to -6,2 ^{0}C, is associated with the 2-VP homopolymer, Mw from 1250 up to 1300 amu, and the copolymer EGDMA-2-VP with Mw in the range of 4200 up to 4300 amu, Fig. 6A, and Fig. 7A. That temperature range is not associated with the pure residue of EGDMA, as can be seen in Fig. 7B.

The second range, 30.4 up to 34.7 ^{0}C, is associated only with the 2-VP homopolymer with Mw at 1900 up to 2000 amu, Fig. 6A, and Fig. 7C.

The third range, from 122.5 to 129.5 ^{0}C, is associated with the complete final decomposition of EGDMA homopolymer, with a boiling point of about 104 ^{0}C; after that temperature, the reactant became unstable. The temperature range is lower enough to discharge the 2-VP decomposition releasing cyanide fumes and nitrogen oxides (NO and NO$_2$). Neither would it be attributed to the 2-VP residual synthesis components, such as styrene (boiling point of 145 ^{0}C), butadiene (boiling point of -4.4 ^{0}C), isobutylene (boiling point of -6.9 ^{0}C), and methyl-methacrylate (boiling point of 101 ^{0}C).

The fourth range, from 229.8 to 234.6 ^{0}C, is related to the copolymer EDGMA(4):2-VP(1), already identified in the sample, Fig 6A, and Fig 7A. The expected decomposition temperature would be at about 280 ^{0}C for a pure (4:1) copolymer sample. Nevertheless, in residual 2-VP and EGDMA, secondary interactions can occur and eventually other copolymers of EGDMA:2-VP, since they are synthesized in bulk polymerization protocol. The observable phenomenon happens at a temperature higher enough to be compatible with possible different proportions of copolymer decompositions.

4. Conclusions

A comprehensive understanding of the interaction between monomer and template is desirable in molecularly imprinting. The proposed factor (MIF) allows accessing the specific interaction's contribution, involved in the molecularly imprinting. The MIF factor as shown allows obtaining detailed information from the studied system. The result is the specific net effect information over significant system characteristics. The system acid-base behavior is predictable by this information as far as the attractive or repulsive affinities can be understood and controlled. The MIP-14 (EDGMA(4)-2-VP(1)) was the most effective obtained MIP from the experimental combinatory analysis. Based on the combinatory by Box-Behnken experimental design, 14 systems were necessary to achieve the desired result. The Tg study allowed a better understanding of the thermal behavior and X-ray results for the MIP-lumefantrine, as identified as the better performance system by the MIF factor calculation. With the previous use of the MIF factor, the expensive and time-consuming procedure would be avoided. The power to predict the MIP behavior significantly impacts effective laboratory costs, resulting in velocity and hit rate with a simple monomer chemical properties database already available.

References

[1]   B. Sellergren, Direct drug determination by selective sample enrichment on an imprinted polymer, Anal. Chem. 66 (1994) 1578–1582.

[2]   A.M. Rampey, R.J. Umpleby, G.T. Rushton, J.C. Iseman, R.N. Shah, K.D. Shimizu, Characterization of the imprint effect and the influence of imprinting conditions on affinity, capacity, and heterogeneity in molecularly imprinted polymers using the Freundlich isotherm-affinity distribution analysis, Anal. Chem. 76 (2004) 1123–1133.

[3]   C.R.T. Tarley, M.D.P.T. Sotomayor, L.T. Kubota, Polímeros biomiméticos em química analítica. parte 1: preparo e aplicações de MIP (molecularly imprinted polymers) em técnicas de extração e separação, Quim. Nova. 28 (2005) 1076–1086.

[4]   S.S.H. Davarani, A.R. Taheri, N. Rahmatian, Highly selective solid-phase extraction and preconcentration of Azathioprine with nano-sized imprinted polymer based on multivariate optimization and its trace determination in biological and pharmaceutical samples, Mater. Sci. Eng. C. 71 (2017) 572–583.

[5]   M.B. Freitas, P.R. Costa, O.B. Joyce, E.P. Vieira, P.P. Maia, M. Elisa, P.B. Siqueira, Amitriptilina e Nortriptilina em Plasma: Extração em Fase Sólida por Polímeros de Impressão Molecular e Sílica Octadecila para Análise Cromatográfica em Faze Líquida de Alta Resolução, Lat. Am. J. Pharm,[Internet]. 28 (2009) 70–79.

[6]   M. Lasáková, P. Jandera, Molecularly imprinted polymers and their application in solid-phase extraction, J. Sep. Sci. 32 (2009) 799–812.

[7]   P.H.R. da Silva, M.L.V. Diniz, G.A. Pianetti, I. da Costa César, M.E.S.R. e Silva, R.F. de Souza Freitas, R.G. de Sousa, C. Fernandes, Molecularly imprinted polymer for determination of lumefantrine in human plasma through chemometric-assisted solid-phase extraction and liquid chromatography, Talanta. 184 (2018) 173–183.

[8]   A.M. Chrzanowska, A. Poliwoda, P.P. Wieczorek, Characterization of particle morphology of biochanin A molecularly imprinted polymers and their properties as a potential sorbent for solid-phase extraction, Mater. Sci. Eng. C. 49 (2015) 793–798.

[9]   A. Beltran, F. Borrull, R.M. Marcé, P.A.G. Cormack, Molecularly-imprinted polymers: useful sorbents for selective extractions, TrAC Trends Anal. Chem. 29 (2010) 1363–1375.

[10]   D. Bitas, V. Samanidou, Molecular Imprinting for Sample Preparation, LC GC NORTH Am. 36 (2018) 772–776.

[11]   C. Lafarge, M. Bitar, L. El Hosry, P. Cayot, E. Bou-Maroun, Comparison of molecularly imprinted polymers (MIP) and sol-gel molecularly imprinted silica (MIS) for fungicide in a hydro alcoholic solution, Mater. Today Commun. 24 (2020) 101157.

[12]   F.M. de Oliveira, M.G. Segatelli, C.R.T. Tarley, Hybrid molecularly imprinted poly (methacrylic acid-TRIM)-silica chemically modified with (3-glycidyloxypropyl) trimethoxysilane for the extraction of folic acid in an aqueous medium, Mater. Sci. Eng. C. 59 (2016) 643–651.

[13]   L.M. Madikizela, N.T. Tavengwa, L. Chimuka, Applications of molecularly imprinted polymers for solid-phase extraction of non-steroidal anti-inflammatory drugs and analgesics from environmental waters and biological samples, J. Pharm. Biomed. Anal. 147 (2018) 624–633.

[14]   A. Vicario, L. Aragón, C.C. Wang, F. Bertolino, M.R. Gomez, A simple and highly selective molecular imprinting polymer-based methodology for propylparaben monitoring in personal care products and industrial wastewaters, J. Pharm. Biomed. Anal. 149 (2018) 225–233.

[15]   R. Song, X. Hu, P. Guan, J. Li, N. Zhao, Q. Wang, Molecularly imprinted solid-phase extraction of glutathione from urine samples, Mater. Sci. Eng. C. 44 (2014) 69–75.

[16]   Y.-H. Yang, L.-T. Liu, M.-J. Chen, S. Liu, C.-B. Gong, Y.-B. Wei, C.-F. Chow, Q. Tang, A photoresponsive surface molecularly imprinted polymer shell for determination of trace griseofulvin in milk, Mater. Sci. Eng. C. 92 (2018) 365–373.

[17]   D.N. Clausen, J. V Visentainer, C.R.T. Tarley, Development of molecularly imprinted poly (methacrylic acid)/silica for clean-up and selective extraction of cholesterol in milk prior to analysis by HPLC-UV, Analyst. 139 (2014) 5021–5027.

[18]   Y. Nakamura, S. Masumoto, H. Matsunaga, J. Haginaka, Molecularly imprinted polymer for glutathione by modified precipitation polymerization and its application to determination of glutathione in supplements, J. Pharm. Biomed. Anal. 144 (2017) 230–235.

[19] M. Díaz-Álvarez, F. Barahona, E. Turiel, A. Martín-Esteban, Supported liquid membrane-protected molecularly imprinted beads for micro-solid phase extraction of sulfonamides in environmental waters, J. Chromatogr. A. 1357 (2014) 158–164.

[20] A. Koler, T. Gornik, T. Kosjek, K. Jeřabek, P. Krajnc, Preparation of molecularly imprinted copoly (acrylic acid-divinylbenzene) for extraction of environmentally relevant sertraline residues, React. Funct. Polym. 131 (2018) 378–383.

[21] S. Foroughirad, V. Haddadi-Asl, A. Khosravi, M. Salami-Kalajahi, Effect of porogenic solvent in synthesis of mesoporous and microporous molecularly imprinted polymer based on magnetic halloysite nanotubes, Mater. Today Commun. (2020) 101780.

[22] K. Golker, I.A. Nicholls, The effect of crosslinking density on molecularly imprinted polymer morphology and recognition, Eur. Polym. J. 75 (2016) 423–430.

[23] J. Haginaka, H. Tabo, C. Kagawa, Uniformly sized molecularly imprinted polymers for d-chlorpheniramine: Influence of a porogen on their morphology and enantioselectivity, J. Pharm. Biomed. Anal. 46 (2008) 877–881.

[24] L.S. Fernandes, P. Homem-de-Mello, E.C. de Lima, K.M. Honorio, Rational design of molecularly imprinted polymers for recognition of cannabinoids: A structure-property relationship study, Eur. Polym. J. 71 (2015) 364–371.

[25] K.S. Roy, A. Mazumder, D.R. Goud, D.K. Dubey, A simplistic designing of molecularly imprinted polymers for derivative of nerve agents marker using 31P {1H} NMR, Eur. Polym. J. 98 (2018) 105–115.

[26] M.B. de Freitas-Marques, B.C.R. Araujo, P.H.R. da Silva, C. Fernandes, W. da N. Mussel, R. de C. de O. Sebastião, M.I. Yoshida, Multilayer perceptron network and Vyazovkin method applied to the non-isothermal kinetic study of the interaction between lumefantrine and molecularly imprinted polymer, J. Therm. Anal. Calorim. 145 (2021) 2441–2449.

[27] Y.P. Mascarenhas, O Problema da Fase em Cristalografia, J. Exp. Tech. Instrum. 4 (2021) 1–19.

[28] A. Standard, Standard Test Method for Transition Temperatures and Enthalpies of Fusion and Crystallization of Polymers by Differential Scanning Calorimetry, (2015).

[29] J. Bicerano, Prediction of polymer properties, cRc Press, 2002.

[30] D.W. Van Krevelen, K. Te Nijenhuis, Properties of polymers: their correlation with chemical structure; their numerical estimation and prediction from additive group contributions, Elsevier, 2009.

[31] A. Di Carlo, M. Gheorghe, P. Lugli, M. Sternberg, G. Seifert, T. Frauenheim, Theoretical tools for transport in molecular nanostructures, Phys. B Condens. Matter. 314 (2002) 86–90.

[32] M. Elstner, D. Porezag, G. Jungnickel, J. Elsner, M. Haugk, T. Frauenheim, S. Suhai, G. Seifert, Self-consistent-charge density-functional tight-binding method for simulations of complex materials properties, Phys. Rev. B. 58 (1998) 7260.

[33] P. Hohenberg, W. Kohn, Inhomogeneous electron gas, Phys. Rev. 136 (1964) B864.

[34] W. Kohn, L.J. Sham, Self-consistent equations including exchange and correlation effects, Phys. Rev. 140 (1965) A1133.

[35] N. Troullier, J.L. Martins, Efficient pseudopotentials for plane-wave calculations, Phys. Rev. B. 43 (1991) 1993.

[36] L. Kleinman, D.M. Bylander, Efficacious form for model pseudopotentials, Phys. Rev. Lett. 48 (1982) 1425.

[37] J.P. Perdew, K. Burke, M. Ernzerhof, Generalized gradient approximation made simple, Phys. Rev. Lett. 77 (1996) 3865.

[38] S.H. Cheong, S. McNiven, A. Rachkov, R. Levi, K. Yano, I. Karube, Testosterone receptor binding mimic constructed using molecular imprinting, Macromolecules. 30 (1997) 1317–1322.

[39] A. Liu, X. Wang, L. Wang, H. Wang, H. Wang, Prediction of dielectric constants and glass transition temperatures of polymers by quantitative structure-property relationships, Eur. Polym. J. 43 (2007) 989–995.

[40] World Health Organization, The international pharmacopeia [electronic resource], 8th ed., Geneva, 2018.

[41] M.M. Alam, K.S. Jack, D.J.T. Hill, A.K. Whittaker, H. Peng, Gradient copolymers– Preparation, properties and practice, Eur. Polym. J. 116 (2019) 394–414.

[42] F. Danusso, M. Levi, G. Gianotti, S. Turri, End unit effect on the Tg of differentiated series of perfluoro-poly (oxymethylene-co-oxyethylene) oligomers, Eur. Polym. J. 30 (1994) 1449–1455.